Inorganic Chemistry

ARTICLE

pubs.acs.org/IC

# Unusual Dinuclear and Mononuclear Cyclometalated Iridium Complexes of 2,5-Diaryl-1,3,4-oxadiazole Derivatives

Yonghao Zheng, Andrei S. Batsanov, and Martin R. Bryce*

Department of Chemistry, Durham University, South Road, Durham DH1 3LE, U.K.

Supporting Information

**ABSTRACT:** A family of new 2,5-diphenyl-1,3,4-oxadiazole (OXD) derivatives **8**−**11** bearing *ortho*-alkyl substituents on one of the phenyl rings is reported. The reactions of these OXDs with $IrCl_3$ under standard cyclometalating conditions did not give the usual $\mu$-dichloro bridged diiridium OXD complexes. Instead, the novel diiridium complexes **12**−**14** and the monoiridium complex **15** were isolated and characterized by X-ray crystallography. It is proposed that the unusual structures arise because of the *ortho*-alkyl substituents leading to a substantial twisting of part of the OXD system which, for steric reasons, changes the normal course of the metal−ligand coordination reactions. Subsequent reactions of **13** and **15** gave the mononuclear complexes **16**−**18** with acac and picolinate anciliary ligands. The crystal structures of **16** and **18** are reported. Photoluminescence is observed in the green (**16**) and blue-green regions (**17** and **18**) at room temperature. Complexes **16**−**18** are phosphorescent at low temperature, with triplet lifetimes of 4.2−5.7 $\mu$s at 77 K.

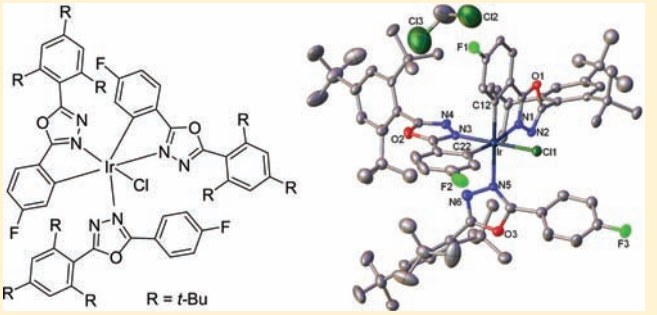


## INTRODUCTION

The synthesis, structural properties, and photophysics of iridium complexes have been extensively studied for many years.[1] Cyclometalated iridium(III) complexes have received special attention for optoelectronic applications, notably as dopants for harvesting the otherwise nonemissive triplet states formed in organic light-emitting devices (OLEDs).[2] The complexes are charge neutral and generally have good chemical and photochemical stability, combined with highly efficient emission from triplet metal-to-ligand charge-transfer ($^3$MLCT) states with ligand-centered ($^3$LC) contributions. Early work on phenylpyridine ligands included the pioneering studies on *fac*-Ir(ppy)$_3$ {*fac*-tris[2-phenylpyridinato]Ir-(III)}[3] and (ppy)$_2$Ir(acac) (acac = acetylacetone)[4] and analogues.[5] Variation of the bidentate C^N cyclometalating ligand has embraced a range of aryl and heteroaryl functionalities.[6−15] Representative examples include homoleptic and/or heteroleptic complexes of 1-phenylisoquinoline,[6,10] 2-phenylquinoxaline,[7] thienylpyridine,[8,10] arylbenzoxazole,[9] naphthylbenzoxazole,[7] benzothienylpyridine,[8,10] thienylisoquinoline,[9] fluorenylpyridine,[9−13] carbazolylpyridine,[14] 1-arylpyrazole,[15] and other ligands of these generic types.

Multiheteroatom ligands have been less widely exploited. Examples include triazole[5,16] and 1,3,4-oxadiazole derivatives.[17,18] The latter are the focus of the present work. 2,5-Diaryl-1,3,4-oxadiazoles (OXDs) are widely used as electron transporting and hole blocking materials in OLEDs because of their moderate electron affinity, high photoluminescence quantum yield, and good thermal and chemical stabilities.[19] However, they have only rarely been used as C^N ligands in cyclometalation reactions. Ma's group reported the X-ray crystal structures and photophysics of mononuclear Ir(III) OXD complexes with an acetylacetone (acac) or dithiolate as the ancillary ligand, for example, **1**, along with the X-ray structure of a standard $\mu$-dichloro bridged diiridium complex **2** (Chart 1).[17] Xu et al. reported related complexes with an acac ligand including the X-ray structure of complex **3**.[18] Moret and Chen have recently characterized a Pt(II) complex of an OXD ligand.[20] We now explore the complexation of OXD derivatives which possess novel substitution patterns.

We report the synthesis of a new series of OXD derivatives **8**−**11** bearing *ortho*-alkyl substituents on one of the phenyl rings and their derived cyclometalated Ir(III) complexes. X-ray crystal structures reveal that dinuclear and mononuclear complexes with very unusual structures are formed under standard cyclometalation conditions as a result of the *ortho*-alkyl substituents inducing steric overcrowding which has profound effects on the course of the metal−ligand coordination reactions.

## EXPERIMENTAL SECTION

**Materials, Synthesis, and Characterization.** All air-sensitive reactions were conducted under a blanket of argon which was dried by passage through a column of phosphorus pentoxide. All commercial chemicals were used without further purification unless otherwise stated. Solvents were dried and degassed following standard procedures. Column chromatography was carried out using 40−60 $\mu$m mesh silica. Melting points were determined in open-ended S2 capilliaries using a Stuart Scientific SMP3 melting point apparatus at a ramping rate of

**Received:** October 26, 2010
**Published:** March 18, 2011

**Chart 1**

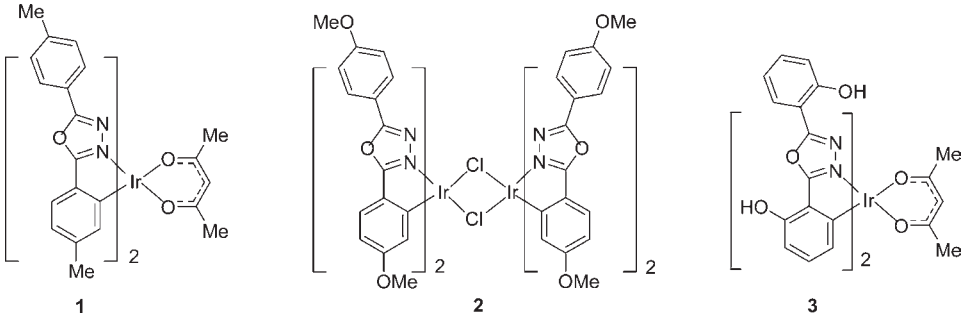


5 °C/min. NMR spectra were recorded on Bruker Avance 400 or Varian VNMRS 700 spectrometers. Chemical shifts are referenced to TMS at 0.00 ppm. Mass spectra were measured on a Waters Xevo OTofMS with an ASAP probe, a Thermoquest Trace or a Thermo-Finnigan DSQ. Elemental analyses were performed on a CE-400 Elemental Analyzer. Absorption spectra were obtained using a Perkin-Elmer Lambda 19 double beam spectrophotometer in 1 cm path length quartz cells. Excitation and emission photoluminescence spectra were recorded on a Horiba Jobin Yvon SPEX Fluorolog FL3−22 spectrofluorometer. Samples were held in quartz fluorescence cuvettes, $l$ = 1 cm ×1 cm, degassed by repeated freeze−pump−thaw cycles until the pressure gauge showed no further movement upon a new pump phase and sealed by way of a Teflon Young's tap. Solutions had $A$ = 0.10−0.15 at 400 nm to minimize inner filter effects. The fluorescence lifetimes were measured by time-correlated single photon counting (TCSPC) using a pulsed diode laser (396 nm) providing a 1 MHz train of pulses of <100 ps. The fluorescence emission was collected at right angles to the excitation source, with the emission wavelength selected using a monochromator and detected by a cooled photomultiplier tube module photon (IBH TBX-04). The instrument response function was measured using a dilute LUDOX suspension as the scattering sample, setting the monochromator at the emission wavelength of the laser, giving an instrument response function (IRF) of 250 ps at 396 nm. The resulting intensity decay was a convolution of the fluorescence decay with the IRF, and iterative reconvolution of the IRF with a decay function and nonlinear least-squares analysis were used to analyze the convoluted data. Phosphorescence measurements were performed using a home-made setup, a $N_2$ laser (337 nm, 10 $\mu$J, 10 Hz) was used as an excitation source. Emission was detected in a 90° geometry by a photomultiplier tube (Hamamatsu R928) as a function of time, selecting a wavelength close to the peak emission by way of a monochromator (Horiba Jobin Yvon Triax 320) with a 0.1−2.0 nm bandpass. The signal was averaged and converted to a digital signal by a digital storage oscilloscope (Tetronix TDS 340). The data were fitted to single exponential functions of the form $I(t) = I_0\exp(-t/\tau)$. Low temperature measurements were conducted using an Oxford Instruments DN1704 optical cryostat.

Cyclic voltammograms were recorded at a scan rate of 100 mV $s^{-1}$ at room temperature using an airtight single-compartment three-electrode cell equipped with a Pt disk working electrode, Pt wire counter electrode, and Pt wire pseudoreference electrode. The cell was connected to a computer-controlled Autolab PG-STAT 30 potentiostat. The solutions contained the complex and $n$-$Bu_4NPF_6$ (0.1 M) as the supporting electrolyte in dichloromethane. All potentials are reported with reference to an internal standard of the decamethylferrocene/decamethyl ferrocenium couple ($FcMe_{10}/FcMe_{10}^+$ = 0.00 V).

**2-(4-Fluorophenyl)-5-(2,4,6-trimethylphenyl)-1,2,4-oxadiazole 8.** A mixture of **6**[21] (0.13 g, 0.80 mmol), 2,4,6-trimethylbenzoyl chloride (0.15 g, 0.80 mmol), and pyridine (5 mL) was refluxed overnight. The solution was cooled, and water was added. The precipitate was collected, dried, and purified by column chromatography ($SiO_2$, eluent DCM:EtOAc, 19:1 v/v) followed by recrystallization from ethanol to yield **8** (0.18 g, 85%) as colorless crystals; mp: 102.2−102.8 °C. Anal. Calcd for $C_{17}H_{15}FN_2O$: C, 72.32; H, 5.36; N, 9.92. Found: C, 72.27; H, 5.30; N, 10.10; $\delta_H$ (700 MHz, $CDCl_3$) 8.09 (2H, dt, $J$ 6.9, 13.9), 7.21 (2H, t, $J$ 8.6), 6.99 (2H, s), 2.35 (3H, s), 2.31 (6H, s); $\delta_C$ (176 MHz, $CDCl_3$) 164.74 (d, $J$ 252.4), 163.91, 141.09, 138.71, 129.10 (d, $J$ 8.9), 128.87, 128.47, 120.95, 120.40 (d, $J$ 3.3), 116.40 (d, $J$ 22.3), 21.27, 20.47; $\lambda_{abs}$ ($CH_2Cl_2$) ($\varepsilon$, $10^4$ $dm^3$ $M^{-1}$ $cm^{-1}$) 264 nm (1.62); MS (EI): $m/z$ 282 ($M^+$, 100%).

**2-(4-Fluorophenyl)-5-(2,4,6-tri-*iso*-propylphenyl)-1,2,4-oxadiazole 9.** Following the procedure for **8**, **6** (1.50 g, 9.1 mmol), 2,4,6-tri-*iso*-propylbenzoyl chloride (2.68 g, 10.0 mmol), and pyridine (10 mL) gave **9** (1.85 g, 55%) as colorless crystals; mp: 119.3−120.6 °C; Anal. Calcd for $C_{23}H_{27}FN_2O$: C, 75.38; H, 7.43; N, 7.64. Found: C, 75.32; H, 7.50; N, 7.60; $\delta_H$ (700 MHz, $CDCl_3$) 8.11−8.06 (2H, m), 7.23−7.19 (2H, m), 7.12 (2H, s), 2.96 (1H, hept, $J$ 6.9), 2.65 (2H, hept, $J$ 6.9), 1.29 (6H, d, $J$ 6.9), 1.21 (12H, t, $J$ 8.2); $\delta_C$ (176 MHz, $CDCl_3$) 164.84 (d, $J$ 218.0), 164.02, 163.86, 152.46, 149.45, 129.08 (d, $J$ 8.8), 121.20, 120.47, 119.56, 116.42 (d, $J$ 22.3), 34.57, 31.47, 24.07, 23.87; $\lambda_{abs}$ ($CH_2Cl_2$) ($\varepsilon$, $10^4$ $dm^3$ $M^{-1}$ $cm^{-1}$) 258 nm (2.49); MS (MALDI+): $m/z$ 367 ($M^+$, 100%).

**2-(4-Fluorophenyl)-5-(2,4,6-tri-*tert*-butylphenyl)-1,2,4-oxadiazole 10.** Following the procedure for **8**, **6** (1.23 g, 7.5 mmol), 2,4,6-*tert*-butylbenzoyl chloride (1.92 g, 6.3 mmol) and pyridine (10 mL) gave a product which was purified by column chromatography ($SiO_2$, eluent DCM) followed by recrystallization from ethanol to afford **10** (1.20 g, 47%) as colorless crystals; mp: 168.9−170.3 °C; Anal. Calcd for $C_{26}H_{33}FN_2O$: C, 76.44; H, 8.14; N, 6.86; Found: C, 76.52; H, 8.02; N, 7.02; $\delta_H$ (700 MHz, $CDCl_3$) 8.14−8.02 (2H, m), 7.25 (2H, s), 7.20 (2H, t, $J$ 8.6), 1.36 (9H, s), 1.18 (18H, s); $\delta_C$ (176 MHz, $CDCl_3$) 165.49, 164.69, 164.06, 163.18, 152.90, 151.51, 129.06, 129.01, 122.19, 117.94, 116.51, 116.39, 37.17, 32.16, 31.23, 15.24; $\lambda_{abs}$ ($CH_2Cl_2$) ($\varepsilon$, $10^4$ $dm^3$ $M^{-1}$ $cm^{-1}$) 257 nm (2.54); (EI): $m/z$ 408 ($M^+$, 100%).

**2-(4-Methoxyphenyl)-5-(2,4,6-tri-*iso*-propylphenyl)-1,2,4-oxadiazole 11.** Following the procedure for **8**, **7**[21] (1.50 g, 9.1 mmol), 2,4,6-tri-*iso*-propylbenzoyl chloride (2.68 g, 10.0 mmol) and pyridine (10 mL) gave **11** (1.85 g, 55%) as colorless crystals; mp: 160.5−161.3 °C; Anal. Calcd for $C_{24}H_{30}N_2O_2$: C, 76.16; H, 7.99; N, 7.40. Found: C, 76.01; H, 7.74; N, 8.60; $\delta_H$ (700 MHz, $CDCl_3$) 8.02 (2H, d, $J$ 8.9), 7.12 (2H, s), 7.02 (2H, d, $J$ 8.9), 3.87 (3H, s), 2.95 (1H, dt, $J$ 7.0, 14.0), 2.67 (2H, hept, $J$ 6.8), 1.29 (6H, d, $J$ 6.9), 1.20 (12H, d, $J$ 6.8); $\delta_C$ (176 MHz, $CDCl_3$) 164.93, 163.28, 162.27, 152.26, 149.46, 128.57, 121.14, 119.88, 116.65, 114.52, 55.45, 34.57, 31.41, 24.08, 23.88; $\lambda_{abs}$ ($CH_2Cl_2$) ($\varepsilon$, $10^4$ $dm^3$ $M^{-1}$ $cm^{-1}$) 270 nm (2.29); MS (AP+): $m/z$ 379 ($M^+$, 100%).

**Complex 12.** A mixture of the ligand **8** (780 mg, 2.8 mmol), iridium chloride (400 mg, 1.1 mmol), and 2-ethoxyethanol/water (10 mL, 3:1 v/v)


dx.doi.org/10.1021/ic102153x |*Inorg. Chem.* 2011, 50, 3354–3362

was stirred at 120 °C overnight. The solid was collected and recrystallized from DCM/hexane to afford **12** (88 mg, 10%) as yellow crystals. Anal. Calcd for $C_{68}H_{56}Cl_2F_4Ir_2N_8O_4$: C, 51.67; H, 3.57; N, 7.09; Found: C, 51.48; H, 3.50; N, 7.14; $\delta_H$ (700 MHz, $CDCl_3$) 7.69 (2H, dd, *J* 2.4, 10.3), 7.35 (2H, dd, *J* 5.6, 8.4), 7.24−7.22 (2H, m), 6.88 (4H, s), 6.86 (2H, s), 6.66 (2H, td, *J* 2.4, 8.5), 6.47 (2H, td, *J* 2.4, 8.5), 6.40 (2H, s), 5.65 (2H, dd, *J* 2.4, 10.9), 2.44 (6H, s), 2.28 (12H, s), 2.18 (12H, s), 1.54 (6H, s); HRMS (MALDI-TOF): calcd for $[C_{68}H_{56}Cl_2F_4Ir_2N_8O_4+H^+]$: 1581.3074. Found: 1581.3049.

**Complex 13.** Following the procedure for **12**, **9** (533 mg, 1.5 mmol), iridium chloride (200 mg, 0.6 mmol) and 2-ethoxyethanol:water (10 mL; 3:1 v/v) gave **13** (230 mg, 40%) as yellow crystals. Anal. Calcd for $C_{92}H_{104}Cl_2F_4Ir_2N_8O_4$: C, 57.64; H, 5.47; N, 5.84; Found: C, 57.48; H, 5.40; N, 5.72; $\delta_H$ (700 MHz, $CDCl_3$) 7.63 (2H, dd, *J* 2.4, 10.1), 7.27 (4H, ddd, *J* 5.7, 8.5, 19.7), 7.13 (2H, s), 7.01 (4H, s), 6.59 (2H, s), 6.51 (2H, td, *J* 2.5, 8.3), 6.47 (2H, td, *J* 2.4, 8.4), 5.52 (2H, dd, *J* 2.4, 10.8), 3.55 (2H, dt, *J* 6.6, 13.4), 2.89 (4H, tt, *J* 6.9, 14.0), 2.16 (4H, dt, *J* 6.8, 13.6), 2.05 (2H, dt, *J* 6.8, 13.6), 1.44 (6H, d, *J* 6.4), 1.30 (12H, d, *J* 6.9), 1.24 (12H, d, *J* 6.9), 1.01 (18H, d, *J* 6.8), 0.96 (12H, d, *J* 6.8), 0.81 (6H, d, *J* 6.8), 0.77 (6H, d, *J* 6.9). HRMS (MALDI-TOF): calcd for $[C_{92}H_{104}Cl_2F_4Ir_2N_8O_4+H^+]$: 1917.6830. found: 1917.6828.

**Complex 14.** Following the procedure for **12**, **11** (280 mg, 0.7 mmol), iridium chloride (115 mg, 0.3 mmol), and 2-ethoxyethanol/water (10 mL, 3:1 v/v) gave **14** (100 mg, 40%) as yellow crystals. Anal. Calcd for $C_{96}H_{116}Cl_2Ir_2N_8O_8$: C, 58.67; H, 5.95; N, 5.70; Found: C, 58.50; H, 5.73; N, 5.76; $\delta_H$ (700 MHz, $CDCl_3$) 7.46 (2H, d, *J* 2.4), 7.18 (4H, dd, *J* 8.4, 11.3), 7.04 (2H, s), 7.00 (4H, s), 6.55 (2H, s), 6.36 (2H, dd, *J* 2.4, 8.3), 6.27 (2H, dd, *J* 2.4, 8.5), 5.35 (2H, d, *J* 2.4), 3.75 (6H, s), 3.41 (2H, dt, *J* 6.7, 13.4), 3.29 (6H, s), 2.90 (2H, dt, *J* 6.9, 13.8), 2.85 (2H, dt, *J* 7.0, 13.9), 2.25−2.14 (6H, m), 1.42 (6H, d, *J* 6.4), 1.28 (12H, t, *J* 7.3), 1.25 (12H, d, *J* 6.9), 1.02 (6H, d, *J* 6.7), 0.99 (24H, t, *J* 7.3), 0.79 (12H, t, *J* 6.5). HRMS (MALDI-TOF): calcd for $[C_{96}H_{116}Cl_2Ir_2N_8O_8+H^+]$: 1965.7630. Found: 1965.7627.

**Complex 15.** Following the procedure for **12**, **10** (640 mg, 1.6 mmol), iridium chloride (230 mg, 0.7 mmol) and 2-ethoxyethanol/water (10 mL, 3:1 v/v) gave **15** (140 mg, 14%) as yellow crystals. Anal. Calcd for $C_{78}H_{97}ClF_3IrN_6O_3$: C, 65.45; H, 7.52; N, 5.45; Found: C, 65.63; H, 7.80; N, 5.31; $\delta_H$ (400 MHz, $CDCl_3$) 8.18−8.05 (3H, m), 7.63 (1H, d, *J* 1.6), 7.54 (1H, d, *J* 1.6), 7.47−7.33 (6H, m), 7.05 (2H, d, *J* 8.7), 6.88−6.78 (1H, m), 6.60−6.49 (1H, m), 6.02 (1H, dd, *J* = 10.2, 2.4), 1.39 (9H, s), 1.38 (9H, s), 1.33 (9H, s), 1.31 (9H, s), 1.18 (9H, s), 1.00 (9H, s), 0.85 (9H, s), 0.81 (9H, s), 0.60 (9H, s). MS (MALDI-TOF) $m/z$ = 1042.3 (M − 408).

**Complex 16.** A mixture of complex **13** (80 mg, 0.04 mmol), acetylacetone (0.1 mL), $Na_2CO_3$ (100 mg, 0.8 mmol), and 2-ethoxyethanol (10 mL) was stirred at 120 °C overnight. The solvent was removed under reduce pressure, and the product was purified by column chromatography ($SiO_2$, eluent DCM/hexane (2:3 v/v) followed by recrystallization from DCM/hexane to give **16** as yellow crystals (50 mg, 61%). Anal. Calcd for $C_{51}H_{59}F_2IrN_4O_4$: C, 59.92; H, 5.82; N, 5.48. Found: C, 59.74; H, 5.93; N, 5.20; $\delta_H$ (700 MHz, $CDCl_3$) 7.58 (1H, dd, *J* 5.5, 8.3), 7.44 (1H, dd, *J* 5.6, 8.3), 7.21 (1H, dd, *J* 2.4, 9.6), 7.11 (2H, s), 7.03 (2H, s), 6.91 (1H, td, *J* 2.4, 8.7), 6.58 (1H, td, *J* 2.5, 8.6), 6.18 (1H, dd, *J* 2.4, 10.1), 5.37 (1H, s), 2.95 (1H, dt, *J* 7.0, 13.9), 2.90 (1H, dt, *J* 6.9, 13.8), 2.74 (2H, hept, *J* 6.9), 2.32 (2H, hept, *J* 6.8, 13.7), 1.88 (6H, d, *J* 3.6), 1.28 (6H, d, *J* 6.9), 1.24 (6H, d, *J* 6.9), 1.17 (12H, d, *J* 6.8), 1.05 (6H, d, *J* 6.8), 1.00 (6H, d, *J* 6.8); $\lambda_{abs}$ ($CH_2Cl_2$) ($\varepsilon$, $10^4$ $dm^3$ $M^{-1}$ $cm^{-1}$) 263 nm (3.80); HRMS (MALDI-TOF): calcd for $[C_{51}H_{59}F_2IrN_4O_4 + H^+]$: 1023.4213.

**Complex 17.** Following the procedure for **16**, **13** (100 mg, 0.05 mmol), picolinic acid (40 mg, 0.5 mmol), $Na_2CO_3$ (55 mg, 0.6 mmol), and 2-ethoxyethanol (10 mL) gave yellow crystals of **17** (30 mg, 28%). Anal. Calcd for $C_{52}H_{56}F_2IrN_5O_4$: C, 59.75; H, 5.40; N, 6.70. Found: C, 59.65; H, 5.48; N, 6.55; $\delta_H$ (700 MHz, $CDCl_3$) 8.25 (1H, d, *J* 7.7), 7.87 (2H, dd, *J* 6.2, 12.2), 7.58 (1H, dd, *J* 5.5, 8.4), 7.54 (1H, dd, *J* 5.4, 8.3), 7.39−7.30 (1H, m), 7.12 (2H, s), 7.10 (2H, s), 6.83−6.75 (1H, m), 6.75−6.70 (1H, m), 6.47 (1H, dd, *J* 2.3, 9.7), 6.43 (1H, dd, *J* 2.3, 9.5), 2.94 (2H, dt, *J* 7.0, 14.0), 2.68 (2H, dt, *J* 6.8, 13.7), 2.54 (2H, dt, *J* 6.8, 13.5), 1.29−1.24 (18H, m), 1.20 (6H, d, *J* 6.8), 1.18 (6H, d, *J* 6.8), 1.12 (6H, d, *J* 6.8); $\lambda_{abs}$ ($CH_2Cl_2$) ($\varepsilon$, $10^4$ $dm^3$ $M^{-1}$ $cm^{-1}$) 243 nm (4.35); HRMS (MALDI-TOF): calcd for $[C_{52}H_{56}F_2IrN_5O_4+H^+]$: 1046.4008. Found: 1046.3987.

**Complex 18.** Following the procedure for **16**, **15** (70 mg, 0.05 mmol), picolinic acid (50 mg, 0.5 mmol), $Na_2CO_3$ (55 mg, 0.6 mmol), and 2-ethoxyethanol (10 mL) gave yellow crystals of **18** (40 mg, 69%). Anal. Calcd for $C_{58}H_{68}F_2IrN_5O_4$: C, 61.68; H, 6.07; N, 6.20. Found: C, 61.75; H, 6.16; N, 6.02; $\delta_H$ (700 MHz, $CDCl_3$) 8.18 (1H, d, *J* 7.8), 8.07 (1H, d, *J* 5.3), 7.88 (1H, td, *J* 1.4, 7.7), 7.56 (1H, dd, *J* 5.3, 8.4), 7.53−7.43 (6H, m), 7.38−7.33 (1H, m), 6.87 (1H, td, *J* 2.4, 8.6), 6.64 (1H, td, *J* 2.4, 8.6), 6.12 (1H, dd, *J* 2.4, 9.9), 1.35 (9H, s), 1.30 (9H, s), 1.25 (9H, s), 1.11 (18H, s), 0.71 (9H, s); $\lambda_{abs}$ ($CH_2Cl_2$) ($\varepsilon$, $10^4$ $dm^3$ $M^{-1}$ $cm^{-1}$) 256 nm (4.30); HRMS (MALDI-TOF): calcd for $[C_{58}H_{68}F_2IrN_5O_4+H^+]$: 1130.4977. Found: 1130.4927.

**X-ray Crystallography.** Single-crystal X-ray diffraction experiments (Table 1) were carried out on Bruker 3-circle diffractometers with CCD area detectors SMART 1000 (**14**, **16**, **18**) or SMART 6000 (**12**, **13**, **15**), using graphite-monochromated Mo-$K_\alpha$ radiation ($\lambda$=0.71073 Å) and Cryostream (Oxford Cryosystems) open-flow $N_2$ cryostats. The structures were solved by Patterson method and refined by full-matrix least-squares on $F^2$ of all data, using SHELXTL 6.14[22] and OLEX2 software.[23] Full crystallographic data, excluding structure factors, have been deposited at the Cambridge Crystallographic Data Center.

The diffraction of **12** was weak (mean $I/\sigma(I)$ = 5.3, almost no observed reflections with $d$ < 0.9) and showed a pseudo *I*-centered pattern, reflections with odd $h + k + l$ having the mean intensity of about 14% of the overall average. In fact, the structure can be solved in the space group $I2/m$ and refined (with disordered model) to $R_1$ = 0.13. Although the lattice parameters suggest a pseudomerohedral twin law (−1 0 0/0 −1 0/1 0 1) giving the transformed cell $a$ = 12.123, $b$ = 14.384, $c$ = 20.330 Å, $\alpha = \gamma = 90°$, $\beta$ = 107.86°, no satisfactory correction could be achieved on this model. The DMSO molecule of crystallization is disordered [except the O(3) atom] between positions A and B with occupancies 0.535(4) and 0.465(4), respectively. ADP ellipsoids of *all* atoms of the host molecule (though not of the DMSO) are elongated in the same direction, not consistent with any reasonable libration model but pointing toward the solvent-occupied cavity. This can be attributed either to a whole-molecule translational disorder (related to the DMSO disorder) or to incommensurate modulation which could not be rationalized, although some reflections indeed show shoulders or weak satellite peaks which could be tentatively attributed to it. **18**·$CH_2Cl_2$ also gave few observed reflections with $d$ < 0.9, notwithstanding strong diffraction at low angles.

## RESULTS AND DISCUSSION

**Synthesis.** The OXD ligands **8**−**11** were synthesized in moderate to high yields, starting from benzonitrile derivatives **4** and **5**, following the tetrazole route[24] via **6** and **7**, as shown in Scheme 1. The OXD ligands were then reacted with iridium chloride under standard conditions[25] (step iii) for forming a bridged $\mu$-dichloro-bridged diiridium C^N ligand complex (e.g., complex **2**). These reactions did not follow the usual course. Instead, the diiridium complexes **12**−**14** were obtained from **8**, **9**, and **11**, respectively, and the monoiridium complex **15** was obtained from **10**. Presumably, the substantial twisting of part of the OXD system caused by the *ortho*-alkyl substituents leads to steric overcrowding which inhibits the normal course of the metal−ligand coordination reactions, to the

**Table 1. Crystal Data of 12−16 and 18 at $T$ = 120(2) K**

| | 12 | 13 | 14 | 15 | 16 | 18 |
|---|---|---|---|---|---|---|
| CCDC deposition no. | 797526 | 797527 | 797528 | 797529 | 797530 | 797531 |
| chemical formula | $C_{68}H_{56}Cl_2F_4Ir_2N_8O_4 \cdot 2C_2H_6OS$ | $C_{92}H_{104}Cl_2F_4Ir_2N_8O_4 \cdot 2CH_2Cl_2$ | $C_{96}H_{116}Cl_2Ir_2N_8O_8$ | $C_{78}H_{97}ClF_3IrN_6O_3 \cdot CH_2Cl_2$ | $C_{51}H_{59}F_2IrN_4O_4$ | $C_{58}H_{68}F_2IrN_5O_4 \cdot CH_2Cl_2$ |
| formula mass | 1736.76 | 2086.98 | 1965.27 | 1536.19 | 1022.22 | 1214.30 |
| crystal system | monoclinic | monoclinic | triclinic | triclinic | monoclinic | monoclinic |
| $a$/Å | 12.1234(5) | 14.2350(5) | 13.5500(13) | 11.4361(4) | 21.6433(13) | 30.483(2) |
| $b$/Å | 14.3842(5) | 15.2472(5) | 14.5450(14) | 14.8212(5) | 25.9737(15) | 15.1691(11) |
| $c$/Å | 20.2257(9) | 21.7641(8) | 23.775(2) | 23.5183(8) | 17.6713(11) | 27.432(2) |
| α/deg | 90 | 90 | 86.780(7) | 97.025(8) | 90 | 90 |
| $\beta$/deg | 106.922(8) | 100.029(5) | 82.395(7) | 95.160(8) | 110.653(6) | 112.720(14) |
| $\gamma$/deg | 90 | 90 | 70.489(6) | 108.059(8) | 90 | 90 |
| $V$/Å$^3$ | 3374.4(2) | 4651.6(3) | 4377.3(7) | 3726.8(2) | 9295.6(10) | 11700(2) |
| space group (no.) | $P2_1/n$ (# 14) | $P2_1/n$ (# 14) | $P\bar{1}$ (# 2) | $P\bar{1}$(# 2) | $P2_1/c$ (# 14) | $C2/c$ (# 15) |
| $Z$, $\mu$/mm$^{-1}$ | 2, 4.15 | 2, 3.09 | 2, 3.16 | 2, 1.96 | 8, 2.93 | 8, 2.43 |
| crystal size, mm | 0.21 × 0.11 × 0.09 | 0.50 × 0.28 × 0.14 | 0.22 × 0.11 × 0.10 | 0.36 × 0.16 × 0.06 | 0.20 × 0.17 × 0.08 | 0.46 × 0.15 × 0.04 |
| transmission factor range | 0.613−0.767 | 0.329−0.676 | 0.339−0.746 | 0.643−0.904 | 0.549−0.746 | 0.422−0.746 |
| no. of reflections total | 30989 | 97915 | 51881 | 45991 | 110909 | 41258 |
| no. of unique reflections | 5970 | 16837 | 24151 | 13143 | 24692 | 10305 |
| $R_{int}$ | 0.072 | 0.045 | 0.037 | 0.076 | 0.069 | 0.071 |
| $R_1$, $wR_2$[a,b] | 0.033, 0.086 | 0.030, 0.071 | 0.043, 0.105 | 0.046, 0.129 | 0.040, 0.087 | 0.050, 0.133 |

[a] $R_1 = \Sigma||F_o| - |F_c||/\Sigma|F_o|$ for data with $I > 2\sigma(I)$. [b] $wR_2 = \{\Sigma[w(F_o^2 - F_c^2)^2]/\Sigma[w(F_o^2)^2]\}^{1/2}$ for all data.



dx.doi.org/10.1021/ic102153x |Inorg. Chem. 2011, 50, 3354–3362

**Scheme 1. Reagents and Conditions**[a]

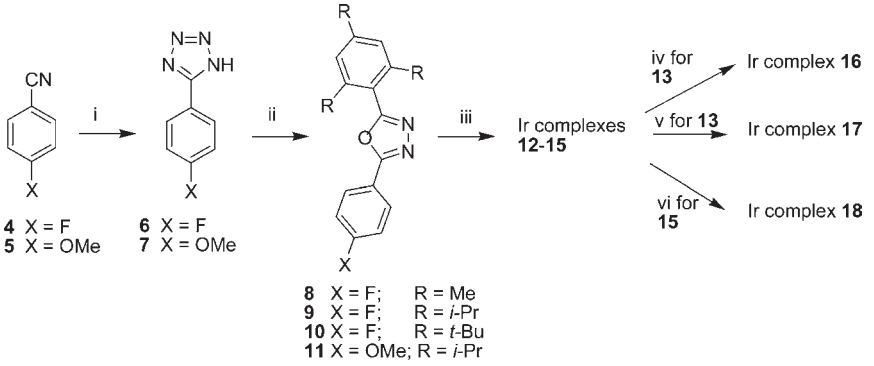


[a] (i) ref 21 for **6** and **7**; (ii) arylbenzoyl chloride, pyridine, reflux; (iii) $IrCl_3$, 2-ethoxyethanol, water, 120 °C; (iv) **13**, acetylacetone, $Na_2CO_3$, 2-ethoxyethanol, 120 °C; (v) **13**, picolinic acid, $Na_2CO_3$, 2-ethoxyethanol, 120 °C; (vi) **15**, picolinic acid, $Na_2CO_3$, 2-ethoxyethanol, 120 °C.

**Chart 2**

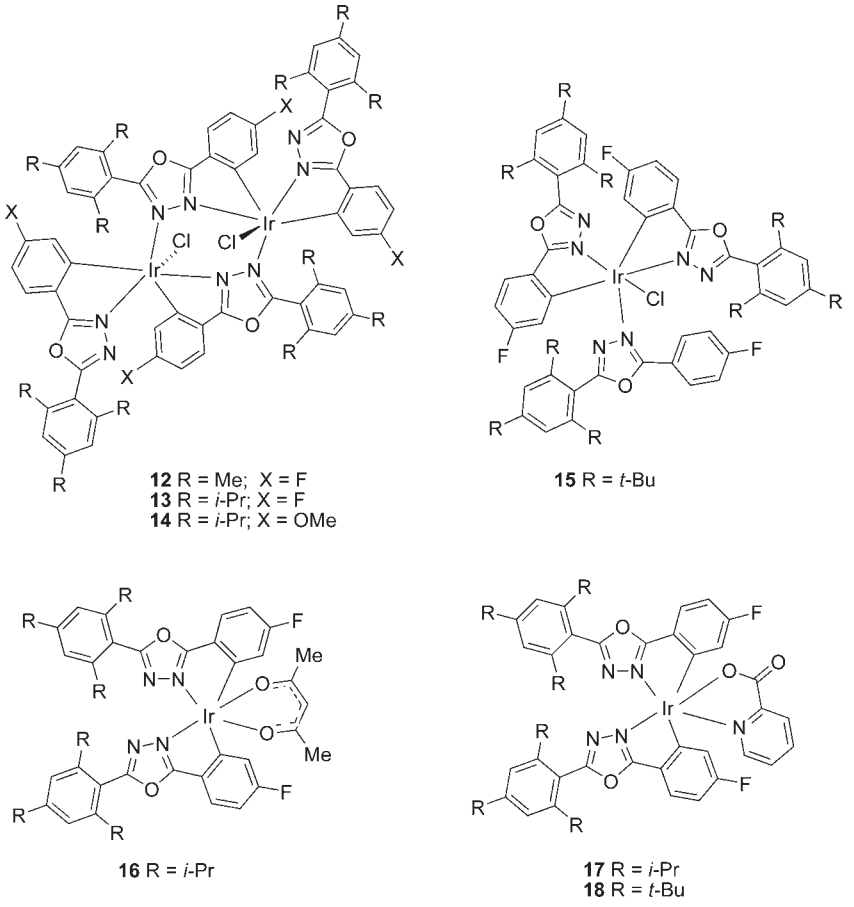


extent that for **10**, which is the bulkiest ligand, the formation of a diiridium complex is precluded altogether. Subsequent reactions of **13** with acetylacetone and picolinic acid and **15** with picolinic acid yielded the acetylacetonate (acac) complex **16** and picolinate (pic) complexes **17** and **18**, respectively. The structures of the complexes **12**−**18**, which are shown in Chart 2, were established by $^1$H NMR spectroscopy, mass spectrometry, and X-ray crystallography (for **12**−**16** and **18**).

**Crystal Structures.** In all the complexes, iridium atoms adopt distorted octahedral coordination. Complexes **12**, **13**, and **14** have similar dimeric structures (Table 2). The structure of **13** is shown in Figure 1; the structures of **12** and **14** are shown in the Supporting Information. Complexes **12** and **13** crystallize with broadly similar crystal lattices and packing motifs, the asymmetric unit comprising half of the dimer (which lies at a crystallographic inversion center) and one solvent molecule (DMSO in


dx.doi.org/10.1021/ic102153x |*Inorg. Chem.* 2011, 50, 3354–3362

**Table 2. Selected Bond Distances (Å) in Complexes 12−14**

| | 12 | 13 | 14, Ir(1) | 14, Ir(2) |
|---|---|---|---|---|
| Ir−Cl | 2.347(1) | 2.3545(6) | 2.356(1) | 2.353(1) |
| Ir−N(1) | 2.175(5) | 2.172(2) | 2.160(3) | 2.166(3) |
| Ir−N(2′) | 2.177(4) | 2.159(2) | 2.175(3) | 2.184(3) |
| Ir−N(3) | 2.033(4) | 2.003(2) | 2.020(3) | 2.026(3) |
| Ir−C (*a*) | 2.023(5) | 2.025(2) | 2.030(4) | 2.028(4) |
| Ir−C (*b*) | 2.035(6) | 2.025(2) | 2.028(4) | 2.037(4) |
| Ir···Ir | 4.299 | 4.298 | 4.313 | |

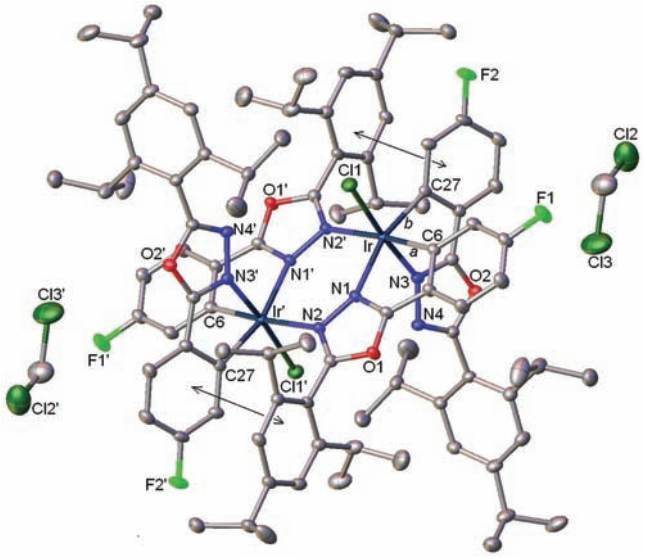


**Figure 1.** Molecular structure of **13**·2$CH_2Cl_2$ (thermal ellipsoids at 50% probability level, disorder and all H atoms are omitted). Primed atoms are generated by the inversion center. Arrows show intramolecular $\pi-\pi$ stacking interactions.

**12** or DCM in **13**), whereas the unsolvated crystal of **14** has one independent molecule in a general position (and is pseudocentrosymmetric). There are four OXD ligands in each complex. Two of the ligands chelate the Ir atom in a bidentate C,N-fashion, whereas two of the ligands are tridentate, chelating one Ir atom in the same C,N-fashion and coordinating the other Ir via the remaining nitrogen atom. The chloro ligands are terminal; thus **12**−**14** differ from the diiridium OXD complexes known previously, all of which have $[(OXD)_2Ir]_2(\mu\text{-}Cl)_2$ type structures with two chloro-bridges.[17] Complex **15** (crystallized as DCM monosolvate, Figure 2) is mononuclear, with two N,C-chelating and one N-monodentate OXD ligand and one terminal chloro ligand. Hence it can be regarded as analogous to the monomeric units of **12**−**14**, except for the monodentate OXD being coordinated through a different nitrogen atom. In each OXD ligand, the tri-R-aryl ring is twisted with respect to the oxadiazole ring because of steric overcrowding, the interplanar angle $\tau$ varying from 63 to 88°. The angle ($\varphi$) between the planes of the oxadiazole and the metalated aryl rings is negligible in **12**, **13**, **15** and one bridging ligand of **14**; three other ligands of the latter display a substantial folding (rather than twist) of about 12°, while the monodentate OXD ligand in **15** is twisted with $\varphi$ = 60.5°. In each of the dimers, the two bridging aryloxadiazole moieties and the Ir atoms are roughly coplanar, and there are two

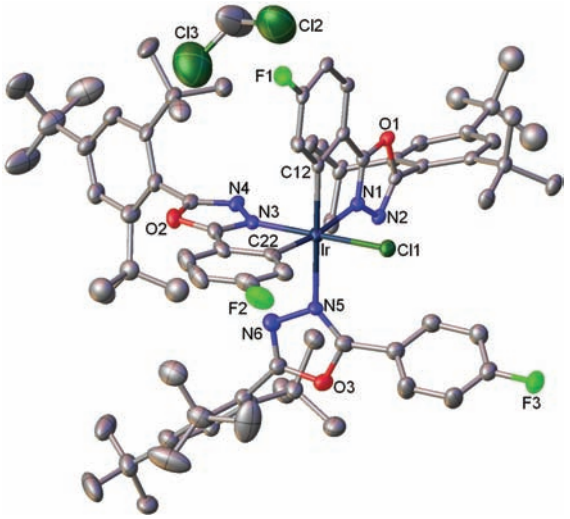


**Figure 2.** Molecular structure of **15**·$CH_2Cl_2$ (thermal ellipsoids at 30% probability level, disorder and all H atoms are omitted). Selected bond distances (Å): Ir−Cl(1) 2.357(1), Ir−N(1) 2.131(4), Ir−N(3) 2.019(4), Ir−N(5) 2.192(4), Ir−C(12) 2.033(5), Ir−C(22) 2.020(6).

cases of intramolecular $\pi-\pi$ stacking (see Figure 1) between a tri-R- and a 4-X-substituted aryl unit, with the interplanar angles of 6° (**12**), 17°(**13**), 10° and 17° (**14**) and the mean interplanar separations of 3.32, 3.43, 3.40, and 3.55 Å, respectively.

Although the N,N′-bridging coordination of OXD has been observed before (in Co, Mn, Re, Cu, Ag, though never in Ir[26] complexes), the only known example of such bridging combined with cyclometalation is (2,5-diphenyl-1,3,4-oxadiazole)-$[Mn(CO)_4]_2$ where *both* metal atoms are C,N-chelated.[27] Diiridium complexes with N,N′-bridging pyrazolyl ligands are well-known, but most of these contain a direct metal−metal bond.[21] In $[\{IrH(O_2CCF_3)(CNBu^t)_2\}_2(\mu\text{-}pz)_2]$ and $[\{(PhO)_3PIrH(Cl)(CO)\}_2(\mu\text{-}pz)_2]$[28] where octahedral, 18-electron iridium(III) centers are bridged by two N,N′-pyrazolyl rings, the $Ir_2(pz)_2$ moiety adopts a folded (butterfly) conformation with the Ir···Ir distances (3.803 and 3.770 Å, respectively) much shorter than in **12**−**14**.

The asymmetric unit of **16** comprises two independent molecules (denoted as molecule *A* and molecule *B*) with the same coordination mode (comprising two C,N-chelating OXD and one acac ligand) but substantially different conformations. The structure of molecule A is shown in Figure 3 and in the Supporting Information, Figure S8. The cyclometalated aryloxadiazole ligand (marked *L1* in Figure 3) is folded in molecules A ($\varphi$ = 15.6°) and both folded and twisted in B ($\varphi$ = 10.0°). The other ligand (marked *L2* in Figure 3) is twisted in both molecules, but the $\varphi$ angles are rather different in magnitude (14.6 and 7.5°) and of opposite sense. The Ir−N(3) bond is inclined to the oxadiazole plane by 20.2° in molecule A and only 10.8° in B, the iridium atom deviating from that plane by 0.74 and 0.39 Å, respectively. This probably causes this bond to be much longer in A than in B (2.158(3) vs 2.093(3) Å), whereas other bond distances are similar. The Ir-acac metallacycle is folded along the O···O vector by 12.4° (A) or 16.0° (B) in opposite directions. Complex **18** (crystallizing as a DCM monosolvate) has a similar conformation mode with the replacement of O,N- for O,O-acac chelation (Figure 4). It shows weaker distortions with $\varphi$ = 6 and 8°.

**Photophysical and Electrochemical Properties.** Photophysical data are shown in Table 3. The absorption and emission


dx.doi.org/10.1021/ic102153x |*Inorg. Chem.* 2011, 50, 3354–3362

spectra of complexes **16**−**18** and the absorption spectra of ligands **9** and **10** in oxygen-free dichloromethane solution are shown in Figure 5. The complexes show strong absorption bands in the 250−300 nm region which are assigned[8] to ligand-centered $\pi-\pi^*$ transitions and closely resemble the absorption spectra of the free ligands **9** and **10**. The complexes show absorption bands with lower extinction in the range 300−425 nm which are ascribed to singlet and triplet metal-to-ligand charge-transfer ($^1$MLCT and $^3$MLCT) states, following literature precedents[8] and the calculations of Hay.[29] It is not possible to distinguish the singlet and triplet absorptions, although the precedent is that the lower energy bands are predominantly triplet in character.

Luminescence in DCM at 293 K, with very low photoluminescence quantum yields (PLQYs), because of nonradiative decay, is observed for **16** ($\lambda_{max}^{em}$ 482(sh), 518 nm), **17** ($\lambda_{max}^{em}$ 471, 496 nm), and **18** ($\lambda_{max}^{em}$ 462 nm) which is visible as green (**16**) and blue-green emission (**17** and **18**). It is well-established for heteroleptic Ir complexes that a pic ancillary ligand leads to blue-shifted emission (usually by ca. 20 nm) compared to the analogous acac complex.[5,7,8] This trend is observed for **17** (pic) compared to **16** (acac). The emission of **18** is blue-shifted in comparison to **17**, which can be explained by reduced conjugation in the OXD ligands of **18**, due to their increased torsion angles, compared to **17** (Figure 6). Lifetime data at 293 K are consistent with the

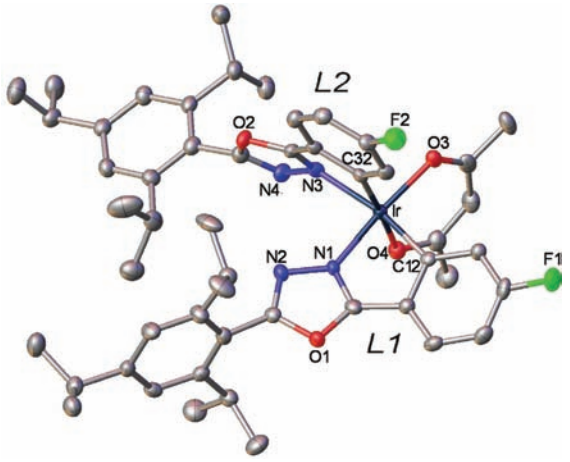


**Figure 3.** Molecular structure of **16** (molecule *A*, thermal ellipsoids at 50% probability level, disorder and all H atoms are omitted). Selected bond distances (Å) in two independent molecules: Ir−O(3) 2.040(2) and 2.040(3), Ir−O(4) 2.118(3) and 2.131(3), Ir−N(1) 1.985(3) and 2.010(3), Ir−N(3) 2.158(3) and 2.093(3), Ir−C(12) 2.006(4) and 2.000(4), Ir−C(32) 2.023(4) and 2.010(4).

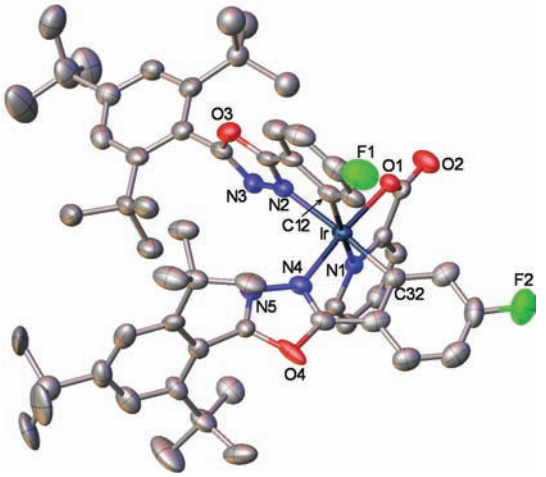


**Figure 4.** Molecular structure of **18** (thermal ellipsoids at 50% probability level, solvent and all H atoms are omitted). Selected bond distances (Å): Ir−O(1) 2.055(4), Ir−N(1) 2.108(5), Ir−N(4) 1.994(5), Ir−N(2) 2.097(6), Ir−C(32) 2.023(7), Ir−C(12) 2.033(7).

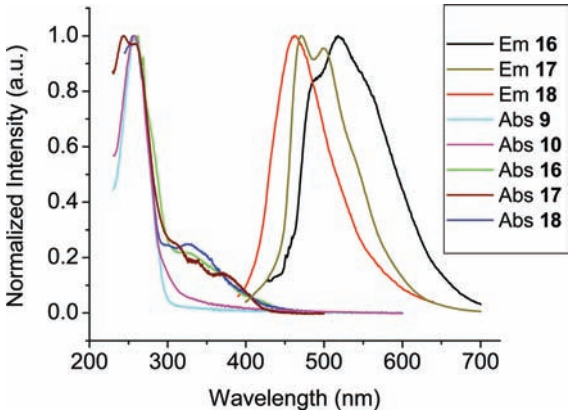


**Figure 5.** Normalized absorption and emission spectra of complexes **16**, **17**, and **18** and absorption spectra of ligands **9** and **10** in oxygen-free dichloromethane solution at 293 K.

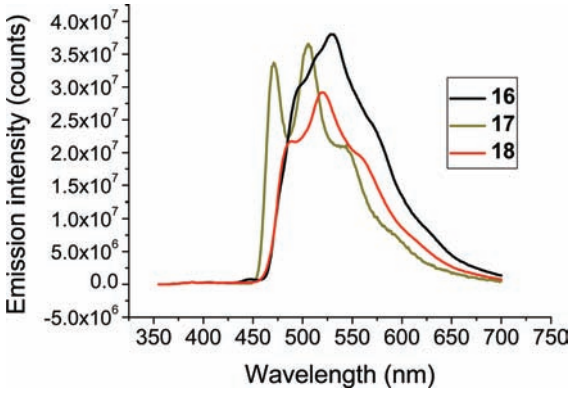


**Figure 6.** Emission spectra of complexes **16**, **17**, and **18** in EPA (a mixture of diethyl ether: 2-methylbutane: ethanol, 5:5:2 v/v) at 77 K.

**Table 3. Photophysical Data**

| complex | $\lambda_{max}^{abs}$/nm (293 K)[a] | $\lambda_{max}^{em}$/nm (293 K)[a] | $\lambda_{max}^{em}$/nm (77 K)[b] | lifetime /$\tau$ (293 K)[b] | lifetime /$\tau$ (77 K)[b] | PLQY, $\Phi$ (293 K)[a,c] |
|---|---|---|---|---|---|---|
| **16** | 263 | 482(sh), 518 | 496(sh), 529, 574(sh) | 3.8 $\mu$s[d] | 4.6 $\mu$s | <0.01 |
| **17** | 243 | 471, 496 | 470, 504, 543(sh) | 0.3 $\mu$s[d] | 4.2 $\mu$s | <0.01 |
| **18** | 256 | 462 | 483(sh), 519, 563(sh) | 6.3 ns | 5.7 $\mu$s | <0.01 |

[a] Measured in $CH_2Cl_2$ solution, $\lambda^{ex}$ 350 nm. [b] Measured in EPA. [c] Measured using an integrating sphere. [d] A fluorescent component with a lifetime in the nanosecond region was also observed.


dx.doi.org/10.1021/ic102153x |*Inorg. Chem.* 2011, 50, 3354–3362

following emission features: for **16** and **17** emission is a combination of fluorescence and phosphorescence; for **18** only fluorescence is observed, with an excited state lifetime in the nanosecond regime. The increased vibronic fine structure for **16** and **17** at 293 K is consistent with a combination of $^3$MLCT states and LC $^3\pi-\pi^*$ transitions.[8] At 77 K strong phosphorescence is observed for all three complexes; the spectra show the characteristic vibronic fine structure. Excited state lifetimes at 77 K are all in the microsecond regime. Such long-lived excited states suggest that the emitting state has triplet character. The luminescence decay profiles are shown in the Supporting Information. Further photophysical studies on these and analogous complexes will be undertaken to probe the interesting interplay of fluorescence and phosphorescence.

The electrochemical properties of **16** and **18** were studied by cyclic voltammetry in dichloromethane solution which established that each complex has a quasi-reversible single-wave oxidation ascribed to a metal-centered $Ir^{3+}/Ir^{4+}$ process at $E^{ox}$ 1.28 V (**16**) and 1.50 V (**18**) in dichloromethane versus $FcMe_{10}/FcMe_{10}^+$ (see Supporting Information).

## CONCLUSIONS

The significance of this work is that we have established that steric factors on the cyclometaling ligand can lead to organoiridium complexes with novel and unexpected structures. Reactions of OXD derivatives **8**−**11**, bearing *ortho*-alkyl substituents on one of the phenyl rings, with iridium chloride under standard conditions do not lead to the usual $\mu$-dichloro-bridged diiridium C^N ligand complexes. Instead, the dinuclear complexes **12**−**14** and mononuclear complex **15** have been isolated and characterized crystallographically. Subsequent reactions of **13** and **15** gave the mononuclear complexes **16**−**18** with acac and picolinate anciliary ligands. Luminescence for **16** ($\lambda_{max}^{em}$ 482(sh), 518 nm) and **17** ($\lambda_{max}^{em}$ 471, 496 nm) and **18** ($\lambda_{max}^{em}$ 462 nm) is observed in DCM at room temperature in the green (**16**) and blue-green regions (**17** and **18**). Complexes **16**−**18** are phosphorescent at low temperature, with triplet lifetimes of 4.2−5.7 $\mu$s at 77 K. The scope of metal chelation to sterically hindered ligands can now be explored in other luminescent complexes with different metal−ligand combinations in the search for complexes with unusual structural properties.

## ASSOCIATED CONTENT

**Supporting Information.** X-ray crystallographic data including files in CIF format for **12**−**16** and **18**; absorption spectra and luminescence decay profiles; cyclic voltammograms of **16** and **17**. This material is available free of charge via the Internet at http://pubs.acs.org.

## AUTHOR INFORMATION

**Corresponding Author**
*E-mail: m.r.bryce@durham.ac.uk.

## ACKNOWLEDGMENT

We thank Durham University and Thorn Lighting for funding. We thank Robert M. Edkins and Andrew Beeby for assistance with lifetime measurements.

## REFERENCES

(1) Review: Dixon, I. M.; Collin, J.-P.; Sauvage, J.-P.; Flamigni, L.; Encinas, S.; Barigelletti, F. *Chem. Soc. Rev.* **2000**, *29*, 385–391.

(2) Reviews: (a) Holder, E.; Langeveld, B. M. W.; Schubert, U. S. *Adv. Mater.* **2005**, *17*, 1109–1121. (b) Chou, P.-T.; Chi, Y. *Chem.—Eur. J.* **2007**, *13*, 380–395. (c) Wong, W.-Y.; Ho, C.-L. *J. Mater. Chem.* **2009**, *19*, 4457–4482. (d) Flamigni, L.; Barbier, A.; Sabatini, C.; Ventura, B.; Barigelletti, F. *Top. Curr. Chem.* **2007**, *281*, 143–203. (e) Baranoff, E.; Yum, J.-H.; Graetzel, M.; Nazeeruddin, Md. K. *J. Organomet. Chem.* **2009**, *694*, 2661–2670.

(3) Baldo, M. A.; Lamansky, S.; Burrows, P. E.; Thompson, M. E.; Forrest, S. R. *Appl. Phys. Lett.* **1999**, *75*, 4–6.

(4) Adachi, C.; Baldo, M. A.; Thompson, M. E.; Forrest, S. R. *Appl. Phys. Lett.* **2001**, *90*, 5048–5051.

(5) Coppo, P.; Plummer, E. A.; De Cola, L. *Chem. Commun.* **2004**, 1774–1775.

(6) Deaton, J. C.; Young, R. H.; Lenhard, J. R.; Rajeswaran, M.; Huo, S. *Inorg. Chem.* **2010**, *49*, 9151–9161.

(7) Schneidenbach, D.; Ammermann, S.; Debeaux, M.; Freund, A.; Zöllner, M.; Daniliuc, C.; Jones, P. G.; Kowalsky, W.; Johannes, H.-H. *Inorg. Chem.* **2010**, *49*, 397–406.

(8) Lamansky, S.; Djurovich, P.; Murphy, D.; Abdel-Razzaq, F.; Lee, H.-E.; Adachi, C.; Burrows, P. E.; Forrest, S. R.; Thompson, M. E. *J. Am. Chem. Soc.* **2001**, *123*, 4304–4312.

(9) Lee, H.-P.; Hsu, Y.-F.; Chen, T.-R.; Chen, J.-D.; Chen, H.-C.; Wang, J.-C. *Inorg. Chem.* **2009**, *48*, 1263–1265.

(10) Tsuboyama, A.; Iwawaki, H.; Furugori, M.; Mukaide, T.; Kamatani, J.; Igawa, S.; Moriyama, T.; Miura, S.; Takiguchi, T.; Okada, S.; Hoshino, M.; Ueno, K. *J. Am. Chem. Soc.* **2003**, *125*, 12971–12979.

(11) Ostrowski, J. C.; Robinson, M. R.; Heeger, A. J.; Bazan, G. C. *Chem. Commun.* **2002**, 784–785.

(12) Tavasli, M.; Bettington, S.; Bryce, M. R.; Al Attar, H. A.; Dias, F. B.; King, S.; Monkman, A. P. J. *Mater. Chem.* **2005**, *15*, 4963–4970.

(13) Tavasli, M.; Bettington, S.; Perepichka, I. F.; Batsanov, A. S.; Bryce, M. R.; Rothe, C.; Monkman, A. P. *Eur. J. Inorg. Chem.* **2007** 4808–4814.

(14) (a) Bettington, S.; Tavasli, M.; Bryce, M. R.; Beeby, A.; Al-Attar, H.; Monkman, A. P. *Chem.—Eur. J.* **2007**, *13*, 1423–1431. (b) Ho, C.-L.; Wang, Q.; Lam, C.-S.; Wong, W.-Y.; Ma, D.; Wang, L.; Gao, Z.-Q.; Chen, C.-H.; Cheah, K.-W.; Lin, Z. *Chem. Asian J.* **2009**, *4*, 89–103.

(15) Yeh, Y.-S.; Cheng, C.-H.; Chou, P.-T.; Lee, G.-H.; Yang, C.-H.; Chi, Y.; Shu, C.-F.; Wang, C.-H. *ChemPhysChem* **2006**, *7*, 2294–2297.

(16) (a) Orselli, E.; Kottas, G. S.; Konradsson, A. E.; Coppo, P.; Fröhlich, R.; De Cola, L.; van Dijken, A.; Büchel, M.; Herbert Börner, H. *Inorg. Chem.* **2007**, *46*, 11082–11093. (b) Orselli, E.; Albuquerque, R. Q.; Fransen, P. M.; Fröhlich, R.; Janssen, H. M.; De Cola, L. *J. Mater. Chem.* **2008**, *14*, 4579–4590. (c) Lo, S.-C.; Bera, R. N.; Harding, R. E.; Burn, P. L.; Samuel, I. D. W. *Adv. Funct. Mater.* **2008**, *18*, 3080–3090. (d) Lo, S.-C.; Harding, R. E.; Shipley, C. P.; Stevenson, S. G.; Burn, P. L.; Samuel, I. D. W. *J. Am. Chem. Soc.* **2009**, *191*, 16681–16688.

(17) (a) Chen, L.; Yang, C.; Qin, J.; Gao, J.; You, H.; Ma, D. *J. Organomet. Chem.* **2006**, *691*, 3519–3530. (b) Chen, L.; You, H.; Yang, C.; Ma, D.; Qin, J. *Chem. Commun.* **2007**, 1352–1354. (c) Chen, L.; Yang, C.; Li, M.; Qin, J.; Gao, J.; You, H.; Ma, D. *Cryst. Growth Des.* **2007**, *7*, 39–46. (d) Chen, L.; Yang, C.; Qin, J. *Acta Crystallogr.* **2005**, *C61*, m513–m515.

(18) Xu, Z.; Li, Y.; Ma, X.; Gao, X.; Tian, H. *Tetrahedron* **2008**, *64*, 1860–1867.

(19) Reviews: (a) Kulkarni, A. P.; Tonzola, C. J.; Babel, A.; Jenekhe, S. A. *Chem. Mater.* **2004**, *16*, 4556–4573. (b) Hughes, G.; Bryce, M. R. *J. Mater. Chem.* **2005**, *15*, 94–107.

(20) Moret, M.-E.; Chen, P. *Eur. J. Inorg. Chem.* **2010**, 438–446.

(21) Kothari, P. J.; Singh, S. P.; Parmar, S. S.; Stenberg, V. I. *J. Heterocycl. Chem.* **1980**, *17*, 1393–1398.

(22) Sheldrick, G. M. *Acta Crystallogr.* **2008**, *A64*, 112–122.

(23) Dolomanov, O. V.; Bourhis, L. J.; Gildea, R. J.; Howard, J. A. K.; Puschmann, H. *J. Appl. Crystallogr.* **2009**, *42*, 339–341.

(24) Sauer, J.; Huisgen, R.; Sturm, H. J. *Tetrahedron* **1960**, *11*, 241–251.
(25) (a) Nonoyama, M. *Bull. Chem. Soc. Jpn.* **1974**, *47*, 767–768. (b) Sprouse, S.; King, K. A.; Spellane, P. J.; Watts, R. J. *J. Am. Chem. Soc.* **1984**, *106*, 6647–6653.
(26) August 2010 release of the Cambridge Structural Database, see: Allen, F. H.; Taylor, R. *Chem. Soc. Rev.* **2004**, *33*, 463–475.
(27) Michon, C.; Djukic, J.-P.; Pfeffer, M.; Gruber-Kyritsakas, N.; de Cian, A. *J. Organomet. Chem.* **2007**, *692*, 1092–1098.
(28) Tejel, C.; Ciriano, M. A.; Millaruelo, M.; Lopez, J. A.; Lahoz, F. J.; Oro, L. A. *Inorg. Chem.* **2003**, *42*, 4750–4758.
(29) Hay, P. J. *J. Phys. Chem. A* **2002**, *106*, 1634–1641.